University of Baghdad
College of Engineering
JE
JOURNAL OF ENGINEERING

Journal of Engineering

journal homepage: www.joe.uobaghdad.edu.iq

Volume 29 Number 3 March 2023

Stiffness Characteristics of Pile Models for Cement Improving Sandy Soil by Low-Pressure Injection Laboratory Setup

Samir H. Hussein*
Ph.D. Student
Dept. of Civil Engr.
College of Engr. – Univ. of Baghdad
Baghdad - Iraq
s.hussein1901p@coeng.uobaghdad.edu.iq

Mahmood D. Ahmed
Prof., Ph.D.
Dept. of Civil Engr.
College of Engr. – Univ. of Baghdad
Baghdad-Iraq
dr.mahmood.d.a@coeng.uobaghdad.edu.iq

ABSTRACT

Soil improvement has developed as a realistic solution for enhancing soil properties so that structures can be constructed to meet project engineering requirements due to the limited availability of construction land in urban centers. The jet grouting method for soil improvement is a novel geotechnical alternative for problematic soils for which conventional foundation designs cannot provide acceptable and lasting solutions. The paper's methodology was based on constructing pile models using a low-pressure injection laboratory setup built and made locally to simulate the operation of field equipment. The setup design was based on previous research that systematically conducted unconfined compression testing (U.C.Ts.). The soil improvement techniques were investigated by injecting a low-pressure mixture of water and ordinary Portland cement (O.P.C.) with (0.8, 1, and 1.3) W/C ratios. The study revealed the relationship between pile model samples (U.C.Ts.) and W/C ratios. It also showed that the pile model samples' (U.C.Ts.) result decreased from 14 to 12 to 10 MPa, respectively, with an increase in W/C ratios from 0.8 to 1 and 1.3, respectively. Furthermore, the stiffness characteristics of a jet grouting column were calculated based on Mohr's Circles theory, and numerous theoretical approaches obtained the consequences of tensile strength.

Keywords: Sand improvement, Jet grouting, Laboratory setup, Unconfined compression test.

*Corresponding author
Peer review under the responsibility of University of Baghdad.
https://doi.org/10.31026/j.eng.2023.03.11

Article received: 14/10/2022
Article accepted: 31/10/2022
Article published: 01/03/2023

خصائص الصلابه لنماذج الركائز الناتجه عن حقن التربه الرمليه بالسمنت لتحسين خواصها بواسطه جهاز الحقن المختبري للضغوط الواطئه

سمير حسب الله حسين*
طالب دكتوراه
قسم الهندسه المدنيه
كلية الهندسه – جامعة بغداد
بغداد– العراق

محمود ذياب احمد
استاذ، دكتوراه
قسم الهندسه المدنيه
كلية الهندسه –جامعة بغداد
بغداد– العراق

الخلاصة

قلة المتوفر من الاراضي الصالحه للبناء في مراكز المدن جعل من التطورفي تقنيات تحسين التربه الحل المنطقي لتحسين خواص التربه المتوفره لتتلائم والمتطلبات الهندسيه اللازمه لجعل التربه قادره على تحمل المباني والمنشاات التي ستقام عليها ..تعتبر طريقه الحقن البثقي طريقه جديده وبديله لحل مشاكل الترب التي تعاني من مشاكل تقنيه والتي لاتستطيع التصاميم التقليديه للاسس ان توفر لها حلول دائميه ومقبوله. ستراتيجيه البحث تتضمن انشاء نموذج ركائزمن خلال حقن التربه بخليط السمنت والماء بواسطه جهاز الحقن المختبري المصمم لحقن التربه بضغوط واطئه. الجهاز صمم ليحاكي عمليه الحقن الفعليه التي تجري بواسطه المعدات الخاصه للحقن في مواقع العمل حيث تم تصنيعه في الاسواق المحليه اعتمادا على بحوث سابقه .الجهاز صمم ليتماشى مع منهجيه فحص الانضغاط غير المحصور. تم التحقق من عمليه تحسين التربه من خلال حقن التربه بخليط الماء مع السمنت البورتلاندي العادي باستعمال ثلاث نسبه مختلفه من خلط الماء بالسمنت هي (0.8,1,1.3).الدراسه كشفت العلاقه بين مقاومه الانضغاط لنماذج الركائز(U.C.Ts.) مع مختلف نسب خلط الماء بالسمنت (W/C ratios) كما بينت ان قوه الانضغاط لنماذج الركائز تقل من14 الى 12 ثم الى 10 ميكاباسكال مع زياده نسبه خلط الماء بالسمنت من 0.8 الى 1 الى 1.3 على التوالي كذلك تم حساب خصائص الصلابه لهذه الركائزباستخدام دائره مور ونتائج مقاومه الشد المستحصله من عده فرضيات.

الكلمات الرئيسية: تحسين التربه, الحقن البثقي ,الجهاز المختبري, فحص الانضغاط غير المحصور.

1. INTRODUCTION

Numerous ground improvement technologies are available to overcome poor soil site conditions, some of which have been in use for many decades and others that have only recently been established. The advancement of ground improvement methods, products, systems, and engineering tools has resulted in tremendous knowledge. **(Schaefer, et al., 2012).** Integrating available knowledge with several problem-specific and site-specific elements is required to select the most effective ground improvement technique. These are summed up and examined in light of what is needed to make a ground improvement project a success. **(Chu, et al., 2009).** Jet grouting is reinforcing soft ground by mixing cement slurry with the soil. Jet grouting has been widely used for soft-ground modification in many underground projects. It was used to create base seals and buried grout struts for deep excavations, structural support around tunnel eyes at the entrance and exit points of tunnel boring machines, and seal leaking joints in diaphragm walls. **(Wang, et al., 2013). (Ali and**

Yousuf, 2016) investigated the impacts of cement-fly ash grouted sandy soil samples from Karbala, Iraq, to estimate the shear strength parameters and the effect of these grouted materials on the volume of the grouted zone by injecting 51 cm^3 of slurry. Fly ash class (F) was utilized as a filler with cement grout; it was added to the mixture in weight percentages of 10%, 25%, and 40%. A cement-fly ash mixture with three different weights of the water-cement ratio (w/c) (0.11, 2.33, and 4) and the addition of fly ash was used to enhance the soil sample's properties. The results of the experiments showed that shear strength improved as the water-cement ratio decreased. **(Al-Malkee and Ahmed, 2021)** studied the effect of water-cement ratio variation on the mechanical and physical properties of the soil-cement column. The sandy soil was mixed with cement grout in a laboratory using different water-cement ratios ranging from 0.7 to 1.4 to estimate the properties of grouted samples at various water-cement ratios and other curing times. The results demonstrate that the uniaxial compressive strength (UCS) of grouted samples reduces with increasing the water-cement ratio (W/C) of the grout and that the magnitude of the (UCS) increases proportionally to the logarithm of the curing time. The modulus of elasticity (E50) ratio to the maximum UCS value reduces with an increase in the water-cement ratio. This experimental study was performed by utilizing a low-pressure injection laboratory setup designed and locally manufactured with almost the same performance as the field equipment operation but with a reduced footprint and cost. The investigated soil was loose fine sand with a 20 % relative density from Karbala province, improved by this setup using low-pressure injected mixtures of O.P.C. with 0.8, 1, and 1.3 W/C ratios. The laboratory setup was inspired by and based on **(Nikbakhtan, 2015)**. It was made unique by methodically carrying out the U.C.Ts. Program. It confirmed the setup's efficiency in terms of the homogeneity and reproducibility of the low-pressure injected model pile samples. In other words, many laboratory injection trials were performed to determine the most effective ranges of the setup operational parameters. These parameters include injection pressure (kPa) and flow rate (l/min), diameter (mm), and the number of nozzles, as well as lifting/penetrating speed (cm/min) and rotating speed (rpm) of the drilling and injection rod. Grouted cement is an appropriate method for improving the geotechnical properties of the soil. Unfortunately, field conditions rarely allow for a thorough examination of the behavior of the injected soil. As a result, the soil injection technique was replicated in the laboratory. In many cases, the primary goal of the laboratory injection test is to evaluate grout injectability in a specific soil. As a result, some injectability procedures have been proposed. Laboratory injection tests aim to understand the physical or chemical mechanisms that occur as the injected binder permeates the soil. **(Celik, 2019).**
This work aims to evaluate the effectiveness of the jet grouting approach as a realistic solution for improving the stiffness properties of loose sandy soil using the laboratory low-pressure injection setup.

2. GROUTING TECHNIQUES

Grouting is a technique for improving the engineering characteristics of grounds by injecting different cementitious materials into cracks, fissures, and cavities. These materials increase strength and stiffness while lowering hydraulic conductivity. Consequently, grouting has been widely used for various purposes, including expanding the foundation's bearing capacity, improving slope and subsurface structure stability, and reducing liquefaction

susceptibility. **(Danot, et al., 2007).** The measurement of the unconfined compressive strength (U.C.S.) of the grouted sample obtained by coring or sampling from a grouted ground is widely used to identify and judge the quality of the reinforcement or improvement after the injection of grout. These measurements confirm the grouting method for controlling the grout suspension's shape and position in the field. **(Avci and Mollamahmutoğlu, 2016).** On the other hand, coring or sampling is a costly and time-consuming technique for preparing the specimen for an unconfined compression test, and it might even damage the grouted ground. As a result, prior studies have proposed numerous empirical correlations to determine the U.C.S. of grouted sand for quality control. The establishment of empirical U.C.S. calculating formulas is also attractive since it allows for an approximation of the strength of grouted sand before grout is injected into the sand deposit, which in turn aids in the cost-effective design of soil stabilization. **(Markou and Droudakis, 2013).** The present investigation suggests the empirical formula to correlate the U.C.S. of sand grouted with Dr = 20 % by ordinary Portland cement using three (0.8, 1, and 1.3) W/C ratios. The modulus of elasticity and density of grouted sand were correlated with the U.C.S. results.

3. GROUTED COLUMN STRENGTH

The unconfined compressive strength of the grouted column (U.C.S.) is influenced by several variables, such as the water-to-cement ratio (W/C), relative density (or porosity), particle size, mineralogy, fines content, specific surface of both sand and cement, types of grout, and curing period. Other authors proposed the following relationships to predict the U.C.S. of the grouted columns. **(Kaga and Yonekura, 1991)** established the following formula by examining the properties of grouted sand strength via changing the pure grout strength and the density and particle size of sand over a wide range.

$$U.C.S._{grouted\ sand} = B + A \times \left(U.C.S._{pure\ grout}\right)^{n} \quad (1)$$

where: A, B, and n are fitting parameters related to the properties of sand, such as volumetric specific surface, porosity, or relative density. **(Dano, et al., 2004)** proposed the following relationship based on the experimental results of four grains of sand (Fontainebleau sand and three types of alluvial deposits of the Seine River) grouted with micro-fine cement at a relative density of around 78%. The initial series of unconfined uniaxial compression and tensile tests were performed to highlight the effect of the cement-to-water ratio of the grout on the strength of the grouted sands.

$$U.C.S._{grouted\ sand} = 40 \times \left(\frac{W}{C}\right)^{-2} \quad (2)$$

(Sunitsakul, et al., 2012) performed unconfined compressive strength (U.C.S.) tests of cement-stabilized bases for samples collected from several highway construction projects in Thailand. Results from the statistical analysis indicated that the most critical factors affecting the U.C.S. were the soaked C.B.R. (which strongly depends on the packing density of soils) and the water-to-cement ratio of the stabilizing binder.

$$U.C.S. = 0.427 \times \left(\frac{C.B.R.}{W/C}\right)^{0.578} \quad (3)$$

4. MANUFACTURING LOW-PRESSURE INJECTION LABORATORY SETUP

The laboratory low-pressure injection setup (shown in **Fig. 1**), is prepared in the local industrial markets, it consists of the following parts:

- A steel frame consists of hollow square steel tube sections welded together to hold the setup parts and supported by heavy-duty steel swivel caster wheels.
- A mixing tank with a 100-liter capacity **(Fig. 2)** is supplied with a mixing motor connected by a mixing rod ending with a blending blade. The mixing motor has a 0.5 HP motor controlled by three-phase frequency converters to control the mixing speed and mixing rod rotation. A ¾-inch diameter galvanized pipe connects the bottom of the mixing tank to the injection pump that connects the circulating pipeline.
- A drainage valve plug for washing, cleaning, and draining the injecting tank is supplied to the bottom of the mixing tank.
- The injection pump is an open impeller type, usually used for thick fluid pumping (like the injection fluid) with (1 H.P. and 3000 rpm) connected to the mixing tank from one side and the soil-injecting system from the other.
- The pipe system connected to the injecting pump was branched into three branches. The main branch connects the bottom of the mixing tank to the injecting pump (controlled by a gate valve kit and a diaphragm pressure gauge for controlling the fluid injection pressure that ranges from 15 to 25 kPa depending on soil injection depth and requires column diameter). The second branch circulates the surplus grouting fluid to the mixing fluid tank. Moreover, the third part joins a reinforced plastic hose to transmit the injection fluid from the injection pipe (main branch) to the injection system.
- The injection system **(Figs. 2 and 3)** consists of an external steel cylinder, an internal rotating drilling injection rod for fluid injection, a set of O-ring seals, oil seal kits for preventing grouting fluid leakage, and a set of ball bearings.
- The injection rod **(Fig. 3)** is a 65 cm long steel pipe (16 mm external diameter and 6 mm internal diameter). It ended with a 20 mm steel drilling kit and two nozzles with 3 mm openings.
- The lifting and lowering of the platform injection system consist of the following:
  - A 3-phase electric motor is coupled to a gearbox connected to a 30 mm dia. screw shaft with square threads supplied with a large net. This net is welded to an inner box that is slipped into an external box fixed to the frame setup. According to the gearbox reducing speed, the internal steel box (supporting the injection system) slipped (at 0.2 m/min) up and down into an external steel box within a vertically ranged distance limited by limit switches.
  - A three-phase variable speed geared motor with 1 H.P. will rotate the injection rod clockwise and counterclockwise **(Fig. 3)**.
- The three-phase electric control board consists of accessories like electric contactors, overloads, selector switches, phase failure devices, emergency switches, pushbuttons, and all other fittings to control and operate the motors and the grouting pump.

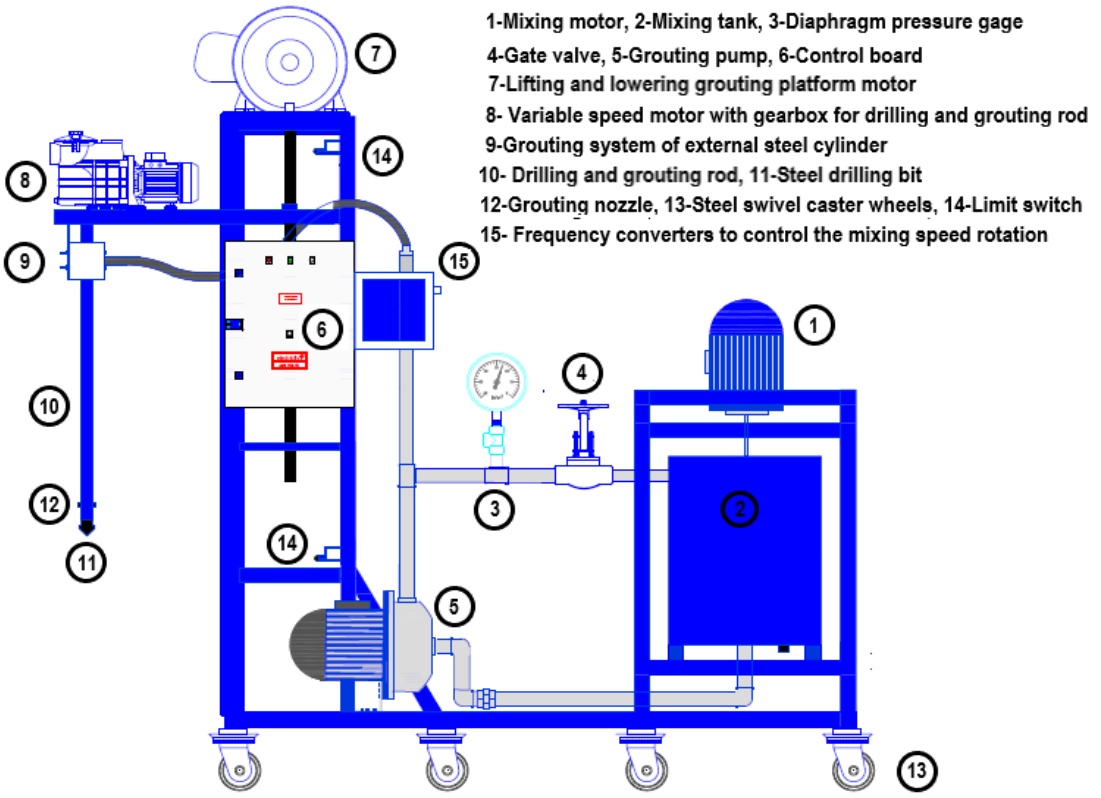

Figure1. Schematic diagram of the laboratory grouting set

Figure 2. Side and Front views of laboratory grouting set

5. PREPARING THE SOIL TESTING BOX

The tested soil in this study is poorly graded sand passing through sieve # 10 (2 mm opening) size **(Fig. 4)**, and its geotechnical characteristics are listed in **Table 1.** The preparation of the soil testing box requires the following steps:

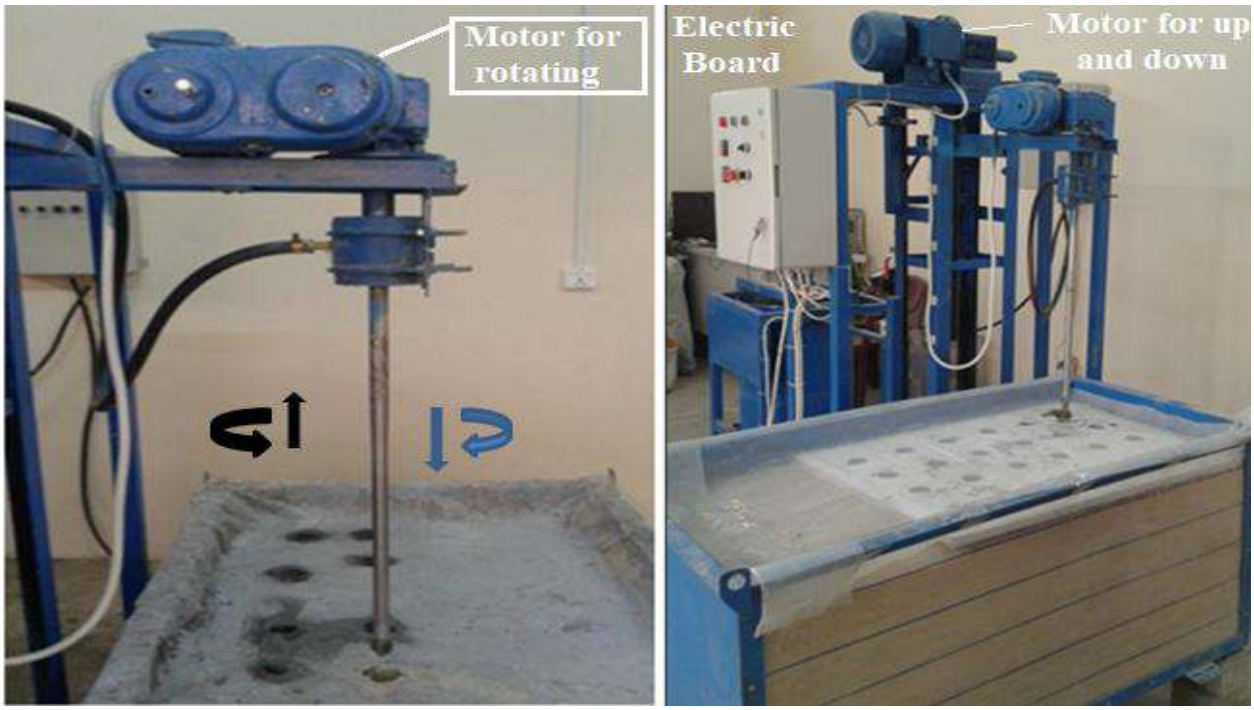

Figure 3. The motion of the grouting rod (up and down) into the sandbox

- The sand in the soil box is spread in layers with a 10 cm height for each layer using the raining (air pluviation) technique **(Lambe and Whitman,1969)** (shown in **Fig. 5**). This technique is used to prepare uniform sand layers for testing large-sized specimens based on laboratory maximum and minimum relative density values (or dry densities) by referring to Eq. (4).

$$D_r = \frac{\gamma_{d\,max.}}{\gamma_d} \times \frac{\gamma_d - \gamma_{d\,min.}}{\gamma_{d\,max.} - \gamma_{d\,min.}} \times 100\% \qquad (4)$$

where; $\gamma_{d\,max.}$ is the dry unit weight in the densest state, $\gamma_{d\,min.}$ is the dry unit weight in the loosest state, and γ_d is the unit weight of the selected soil's density. In this study, it was chosen to have a 20% relative density for laboratory soil specimen preparation (liquefiable sand).

- The weighted dry sand is spread (rained) inside the soil box using a funnel (40 cm diameter and 35 cm height) suspended at 2.5–2.75 m height by a car's engine crane. This high funnel is connected with a 5 cm diameter plastic hose for homogenous sand samples spread within the marked lines drawn on the inner sides of the soil box (made of steel and provided by a polycarbonate transparent front panel).
- After sand rain completion, each layer surface is leveled up (finished by small taping on the layer surface) to the required level marked by lines inside the soil box sides.

- After sandbox preparation, a one-inch thick plastic sandwich panel was applied. It was drilled to the required diameter and number of circles for the columns to be grouted. Then, a thin plastic layer of polythene sheet is placed under this panel to prevent the backflow or spoils (a mixture of grout, water, and sand) from infiltrating the soil during the grouting operation. The polythene sheet layer is punctured during the grouting process, corresponding to the grouted columns' locations.

Table 1. Index Geotechnical Characteristics of sand mixtures

Characteristics of tested sand	Value	Standard or specifications
Soil relative density (D_r %)	20%	According to the study requirements
Max. dry unit weight ($\gamma_{d\,max}$), kN/m^3	18.5	ASTM D4253
Min. dry unit weight ($\gamma_{d\,min}$), kN/m^3	16.8	ASTM D4254
Selected dry unit weight (γ_d), kN/m^3	17.1	Calculated from Eq. (4)
Selected saturated unit weight (γ_{sat}), kN/m^3	20.2	Calculated from soil phase relationships
Specific gravity Gs	2.63	ASTM D854
Max. void ratio e_{max}	0.565	Calculated from soil phase relationships
Min. void ratio e_{min}	0.42	Calculated from soil phase relationship
Depending on the void ratio	0.54	Calculated from soil phase relationship
Uniformity Coefficient (Cu)	2.36	classified as poorly graded
Coefficient of Curvature (Cc)	0.95	The soil is well-graded if the value of Cc lies between 1 and 3
Soil classification USCS	(S.P.)	ASTM D422 and ASTM D2487
Dry friction angle, ø$^\circ$	30	ASTM D3080/ D3080M-11
Saturated friction angle, ø$^\circ_{sat}$	24	Direct shear test/ undrained condition.

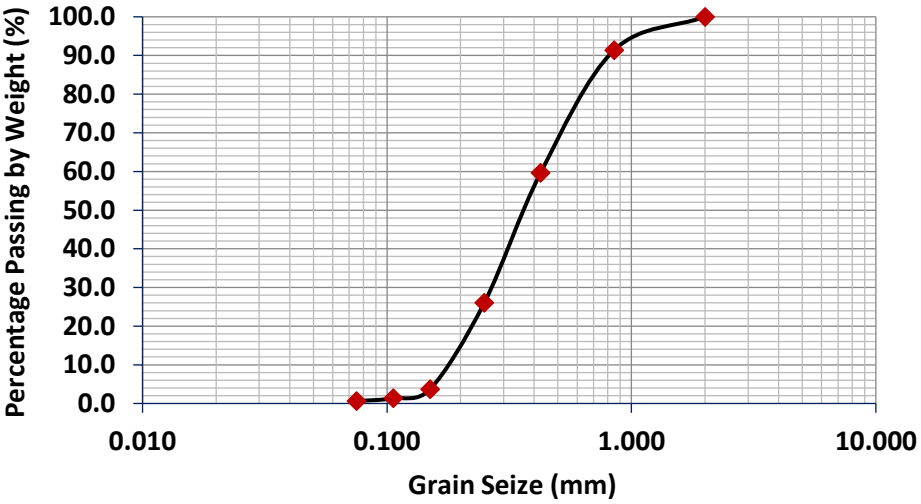

Figure 4. Grain size distribution of selected soil

Figure 5. Soil raining (air pluviation) technique

6. LOW-PRESSURE LABORATORY INJECTING PROCEDURE

After mixing the injection materials (separately in a bucket) according to the required proportions, the injection fluid is poured into the mixing tank in preparation for the injection process which includes the following stages:

- Operate the mixing motor according to the suitable rotation speed from the variable frequency drive inverter on the control board.
- The injection pump is operated by circulating the injection fluid from the bottom of the mixing tank through the pipe system and returning it to the top inlet to ensure the injection pump operates appropriately.
- Then, the drilling injection rod is rotated and lowered into the sandbox.
- Before the injection process, a trial injection pumping (pushing a small amount of injection fluid over the soil surface) is carried out to ensure the proper operation of the nozzle. This initial injection process is vital to guarantee the non-plugging of nozzles (by sand grain intrusion) and injection continuity operation during the soil drilling and injecting process.
- The injecting process is performed on the soil box by directing the platform injecting system downward and rotating (at 50-rpm revolution speed) the drilling and injecting rod in a clockwise direction. The injection process is performed in two stages.

- The first injecting stage is associated with the downward drilling process by injecting the hole with a suitable fluid pressure to stabilize the hole's wall sides.
- The second stage (primary injection process) starts upward after the injection rod reaches the required level in the soil box. From the control board, the rod rotation is reversed in the counterclockwise direction, and the platform grouting system is directed upwardly at the previously prescribed speed with the required injection pressure of pumped fluid according to the diaphragm pressure gauge.

- During the injection process, some spoils flow from the hole surface to be removed from the soil box surface.

- The lifting process for the drilling and injecting system platform continues during the injecting process until the nozzles reach the soil box surface, which is the end of the soil injecting model column performance process that leads to a consistent and homogenous injected column model.
- During the soil injecting process, there is a lowering in the surface area of the injected model columns (local densification for injection leading to shortening of the injected model columns' length) to be substituted with the same soil properties mixed with the upward spoiled injected fluid.
- The injection process continued by moving to another location in the soil box until the required number of model columns were injected **(Fig. 6)**.
- After the injection of model columns, the curing process is started by immersing them in a suitable water basin for a 28-day curing period.

Figure 6. Jet grouting column injection process

Figure 7. Grouted columns diameters

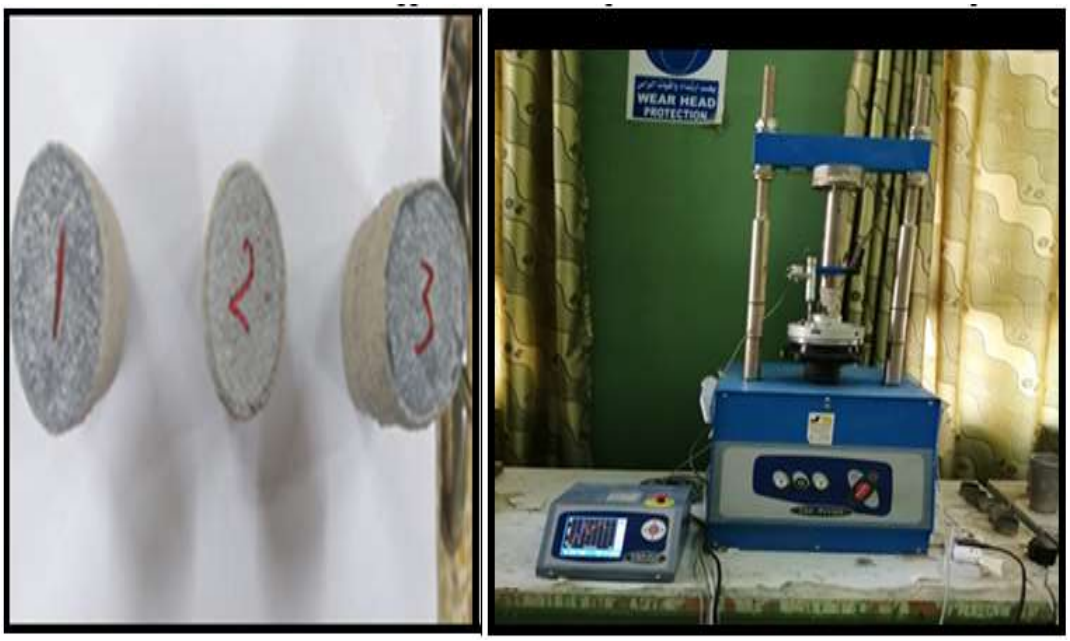

Figure 8. Unconfined Compression Test (U.C.T.) tests

7. UNCONFINED COMPRESSION TEST (U.C.T.) RESULTS

In most experimental work, the unconfined compressive apparatus is employed to study the validity of improving the soil with grouted cement by analyzing the affecting elements. The U.C.T is fundamental for the knowledge of soil cement injection assessment; it is also simple, rapid, trustworthy, and reasonably priced. This study used an unconfined compressive apparatus to test a sample group of low-pressure injected model piles (LPIMPs) **(Fig.s' 7 and 8).** The sample group was randomly selected from (LPIMPs) with (0.8, 1.0, and 1.3) W/C ratios. An automatic loading device with a calibrated load cell and a data logger for data acquisition was used for the experiments. Following **(ASTM D2166, 2006)**, the samples were loaded centrally at a displacement rate of 1.2 mm/min until failure to obtain the maximum applied load. Tests were conducted on identical samples from each W/C group to minimize testing circumstances and material variance. Because the data error was less than 5%, the acquired results were deemed acceptable. Table 2 presents the test results. Using the Curve Expert Professional software version (2.7.3), which generates high-quality results using a cross-platform solution for curve fitting and data analysis, the trend of U.C.S. and the W/C ratio relation for each increasing W/C ratio (**Fig. 9**) exhibited the same behavior as previous studies **(Bruce et al., 2013)** The relation data mathematical modeling has a good coefficient of determination (R^2).

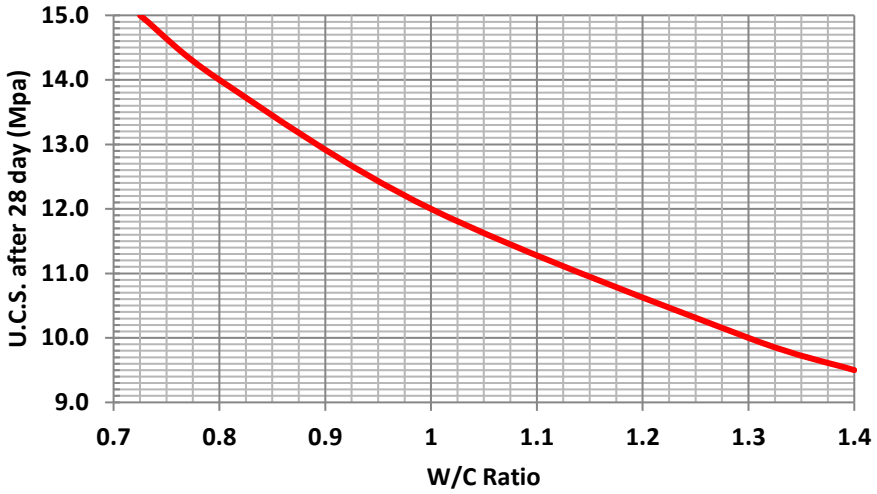

Figure 9. Variation of grouted column's strength and different water-cement ratios

8. JET GROUTING COLUMN PROPERTIES

Determining the compressive strength of a jet grouting column is an essential step in developing jet grouting functions since the cohesion and internal friction angle are utilized to describe the strength properties of jet grouting columns. Various methods have been employed to calculate cohesion and internal friction angles depending on the unconfined compressive strength. One of these approaches is using the relationship between the split tensile and compressive strength data to draw Mohr's circles and failure envelopes and estimate the shear strength parameters. Mohr's Circles can be drawn based on the results of the unconfined compression test for the jet grouted column, as listed in **Table 2**, and the consequences of tensile strength based on numerous theories, as shown in **Table 3**.

Table2. Average unconfined compressive strength with different water-cement ratio

No.	W/C	Average U.C.T. after 28 days of curing (MPa)	Average Elasticity Modulus (MPa)
1	0.8	14	1400
2	1	12	700
3	1.3	10	500

As a result, based on Mohr's Circles theory **(Fig. 10)** and the consequences of tensile strength obtained by numerous theoretical approaches, the shear strength (Cu), internal friction, and other properties of a jet grouting column can be calculated as shown in **Table 4**.

Table3. The results of tensile strength are based on numerous theories.

Average unconfined compressive strength q_u (N/mm^2)			10	12	14
Split Tensile strength (MPa)	**(ACI committee 318, 2014)**	$T = 0.56 \times qu^{0.5}$	1.77	1.94	2.09
	(CEB-FIB, 1991)	$T = 0.3 \times qu^{0.66}$	1.37	1.55	1.71
	(Carino and Lew, 1982)	$T = 0.272 \times qu^{0.71}$	1.395	1.59	1.77
	(Oluokun, et al., 1991)	$T = 0.294 \times qu^{0.69}$	1.44	1.63	1.82
	(Arioglu, et al., 2006)	$T = 0.387 \times qu^{0.63}$	1.65	1.85	2.04
	(Lavanya and Jegan, 2015)	$T = 0.294 \times qu^{0.772}$	1.74	2.0	2.26
	Average T (N/mm^2)		1.56	1.76	1.95

Table 4. The physical properties of produced jet grouting columns

No.	W/C	Av. U.C. S (MPa)	Av. T. S (MPa)	Cohesion (MPa)	Angle of friction	Density (kN/m^3)	Average Elasticity Modulus (MPa)
1	0.8	14	1.95	2.6	49	21	1400
2	1	12	1.76	2.3	48	20.5	700
3	1.3	10	1.56	1.99	47	19.5	500

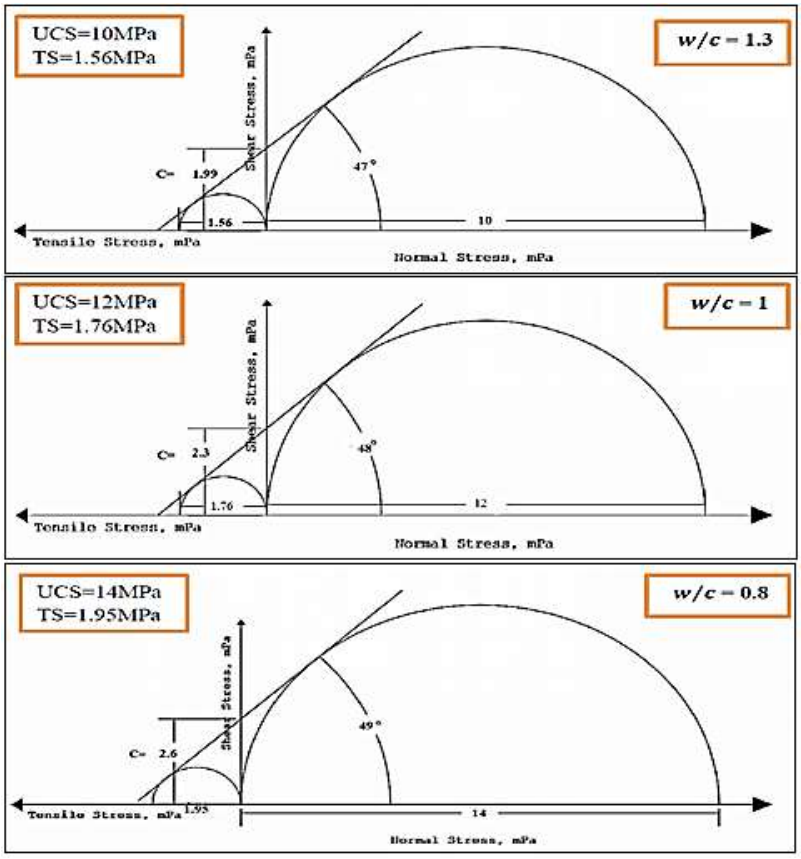

Figure 10. Mohr's Circles and the failure envelop of Jet Grouting Columns.

9. CONCLUSIONS

In certain instances, a preliminary trial for cement injection operations must be conducted on an alternate site with identical soil characteristics to the construction site. Following this trial, the grouted columns are excavated for field inspection and the necessary tests. It is rarely possible to find a location similar to the job site while doing trials of the jet grouting procedure. It could be costly, time-consuming, and not even produce the desired outcomes. Therefore, geotechnical designers must use a low-pressure injection setup to represent the cement grouting improvement technique, so can be concluded the following points from this investigation:

- The primary benefit of designing a low-pressure injection setup is to determine the suitable ranges of the operational injection factors that influence the injection process of an injected binder for enhancing a given soil. These factors include grout pressure and its flow rate, diameter, the number of nozzles, lifting/penetrating speed, and rotating speed of the drilling and injection shaft.
- Depending on injection operating parameters, cement type (or fineness), and binder type, the low-pressure injection laboratory setup is helpful for model improvement for practically all soil types (particularly suitable for sandy soils).
- Methodologically or systematically performing the U.T.Ts. Program on representative samples is critical to validating the process's sample reproducibility and homogeneity.
- In this study, the objective of performing U.C.Ts was to determine the effect of the W/C ratio factor on the strength of low-pressure injected model piles for O.P.C. binders. The result revealed that the trend of the W/C ratios of the O.P.C. binder with U.C.T.s was similar to that of the literate; increasing the W/C ratio leads to decreasing the model plié's strength.
- It can calculate the properties of a jet grouting column based on Mohr's Circles theory and the tensile strength results obtained by numerous theoretical approaches.

Finally, from a sustainable point of view, the cement-water grout technique for improving loose sand can be considered an innovative solution to solve the lack of construction land problem in urban areas.

REFERENCES

ACI committee 318, 2014. *Building code requirements for structural concrete and commentary*, American concrete institute, Farmington Hills, MI, pp. 107.

Ali, H. A., and Yousuf, Y. M., 2016. Improvement of Shear Strength of Sandy Soil by Cement Grout with Fly Ash, *Journal of Engineering*, 22(12), pp. 16–34.

AL-Malkee, F. W., and Ahmed, M. D., 2021. Laboratory Study on the Effect of Water-Cement Ratio on Strength Characteristics of Jet Grouting Columns, *Journal of Engineering*, 27(12), pp. 33–49, doi: 10.31026/j.eng.2021.12.04.

Arioglu, N., Girgin, Z.C., Arioglu, E., 2006. Evaluation of ratio between splitting tensile strength and compressive strength for concretes up to 120 MPa and its application in strength criterion, *ACI Mater. J*. 103 (1), pp. 18–24.

ASTM D422, 63rd Edition, 1972. Standard Test Method for Particle-Size Analysis of Soils.

ASTM D854-14, 2016. Standard Test Methods for Specific Gravity of Soil Solids by Water Pycnometer.

ASTM D.2166, 2006. Standard test method for unconfined compressive strength of cohesive soil.

ASTM D2487-17, 2020. Standard Practice for Classification of Soils for Engineering Purposes (Unified Soil Classification System).

ASTM D3080/D3080M-11, 2020. Standard Test Method for Direct Shear Test of Soils Under Consolidated Drained Conditions.

ASTM D4253-16E1, 2019. Standard Test Methods for Maximum Index Density and Unit Weight of Soils Using a Vibratory Table.

ASTM D4254-00, 2017. Standard Test Methods for Minimum Index Density and Unit Weight of Soils and Calculation of Relative Density.

Avci, E., and Mollamahmutoğlu, M., 2016. UCS properties of superfine cement–grouted sand*, Journal of Materials in Civil Engineering*, 28(12): 06016015,

Bruce, M., Berg, R., Filz, G., Terashi, M., Yang, D., and Collin, J., et al., 2013. Deep mixing for embankment and foundation support, Federal highway administration design manual: Federal Highway Administration. Offices of Research & Development. The United States.

Carino, N.J., and Lew, H.S., 1982. Re-examination of the relationship between splitting tensile and compressive strength of normal weight concrete, *ACI Mater. J.* 79 (3), pp.214–219.

Celik, F., 2019.The observation of permeation grouting method as soil improvement technique with different grout flow models. *Geomechanics and Engineering*; 17(4), pp.367-374.

CEB-FIB Model Code for Concrete Structures, 1991. Evaluation of the Time Dependent Behaviour of Concrete, Bulletin d'Information No. 199, Comite European du Be´ton/Fe´de´ration Internationale de la Precontrainte, Lausanne, pp. 201.

Chu, J., Varaksin, S., Klotz, U., and Mengé, P., 2009. Construction processes. Proceedings of the 17th International Conference on Soil Mechanics and Geotechnical Engineering, Volumes 1, 2, 3, and 4, IOS Press.

Danot, C., and Derache, N., 2007. *Grout injection in the laboratory*, International Symposium on Earth Reinforcement.

Dano, C., Hicher, P. Y., and Tailliez S., 2004. Engineering properties of grouted sands. *Journal of Geotechnical and Geoenvironmental Engineering*, 130(3), pp.328-338.

Kaga, M., and Yonekura, R., 1991. Estimation of the strength of silicate grouted sand, *Soils and foundations*, 31(3), PP. 43-59.

Lambe, T.W., and Whitman, R.V., 1969. *Soil Mechanics*. John Wiley & Sons, New York.p31.

Lavanya, G., and Jegan, J., 2015. Evaluation of the relationship between split tensile strength and compressive strength for geopolymer concrete of varying grades and molarity, *Int. J. Appl. Eng. Res*. 10 (15), pp. 35523–35527.

Markou, I., and Droudakis, A., 2013. Factors affecting engineering properties of microfine cement grouted sands, Geotechnical and Geological Engineering, 31(4), pp.1041-1058.

Nikbakhtan, B., 2015. Development of Thermal-Insulating Soilcrete using Laboratory Jet Grouting Setup, Edmonton, Canada: University of Alberta.

Oluokun, F.A., Burdette, E.G., and Deatherage, J.H., 1991. Splitting tensile strength and compressive strength relationships at early ages, *ACI Mater. J.*, 88 (2), pp. 115–121.

Schaefer, V.R., Mitchell J.K., Berg, R.R., Filz, G.M., and Douglas, S.C., 2012. Ground improvement in the 21st century: a comprehensive web-based information system, Geotechnical Engineering State of the Art and Practice: Keynote Lectures from GeoCongress, pp. 272-293.

Sunitsakul, J., Sawatparnich, A., and Sawangsuriya, A., 2012. Prediction of unconfined compressive strength of soil–cement at seven days, *Geotechnical and Geological Engineering.* 30(1), pp. 263-268.

Wang, Z., Shen, S.L., Ho, C.E., and Kim, Y., 2013. Jet grouting practice: an overview, *Geotechnical Engineering Journal of the SEAGS & AGSSEA*. 44(4), pp.88-96.